Transmembrane Helix 11 of Multidrug Resistance Protein 1 (MRP1/ABCC1): Identification of Polar Amino Acids Important for Substrate Specificity and Binding of ATP at Nucleotide Binding Domain 1†

Da-Wei Zhang,[‡,§] Kenichi Nunoya,[‡,⊥] Monika Vasa,[‡] Hong-Mei Gu,[#] Ashley Theis,[‡,@] Susan P. C. Cole,[‡,@,+] and Roger G. Deeley*[,‡,@,||]

Division of Cancer Biology and Genetics, Cancer Research Institute, and Departments of Pathology and Molecular Medicine, Biochemistry, and Anatomy and Cell Biology, Queen's University, Kingston, K7L 3N6, Canada

Received March 10, 2004; Revised Manuscript Received May 6, 2004

ABSTRACT: Human multidrug resistance protein 1 (MRP1) is an ATP binding cassette (ABC) transporter that confers resistance to many natural product chemotherapeutic agents and can transport structurally diverse conjugated organic anions. MRP1 has three polytopic transmembrane domains (TMDs) and a total of 17 TM helices. Photolabeling and mutagenesis studies of MRP1 indicate that TM11, the last helix in the second TMD, may form part of the protein's substrate binding pocket. We have demonstrated that certain polar residues within a number of TM helices, including Arg^{593} in TM11, are determinants of MRP1 substrate specificity or overall activity. We have now extended these analyses to assess the functional consequences of mutating the remaining seven polar residues within and near TM11. Mutations Q580A, T581A, and S585A in the predicted outer leaflet region of the helix had no detectable effect on function, while mutation of three residues close to the membrane/cytoplasm interface altered substrate specificity. Two of these mutations affected only drug resistance. N597A increased and decreased resistance to vincristine and VP-16, respectively, while S605A decreased resistance to vincristine, VP-16 and doxorubicin. The third, S604A, selectively increased 17β-estradiol 17-(β-D-glucuronide) ($E_2$17βG) transport. In contrast, elimination of the polar character of the residue at position 590 (Asn in the wild-type protein) uniformly impaired the ability of MRP1 to transport potential physiological substrates and to confer resistance to three different classes of natural product drugs. Kinetic and photolabeling studies revealed that mutation N590A not only decreased the affinity of MRP1 for cysteinyl leukotriene 4 (LTC_4) but also substantially reduced the binding of ATP to nucleotide binding domain 1 (NBD1). Thus, polar interactions involving residues in TM11 influence not only the substrate specificity of MRP1 but also an early step in the proposed catalytic cycle of the protein.

Multidrug resistance protein 1 (MRP1/ABCC1)[1] belongs to the C branch of the ATP binding cassette (ABC) superfamily. The human C branch includes MRP1-6 (ABCC1-6) and MRP7-9 (ABCC10-12), as well as the sulfonylurea receptors SUR1 (ABCC8) and SUR2 (ABCC9) and the cystic fibrosis transmembrane conductance regulator CFTR (ABCC7) (*1*−*5*). The predicted topology of MRP1 and several related ABCC proteins differs from that of most eukaryotic ABC transporters, which are composed of two membrane spanning domains (MSDs), each containing six transmembrane (TM) α-helices and connected at their COOH-proximal ends to a cytoplasmic nucleotide binding domain (NBDs) (*6*). MRP1 has an additional NH_2-terminal domain, MSD1, with five TMs and an extracellular NH_2-terminus (*7*, *8*). Thus, MRP1 is predicted to contain three MSDs with 5 + 6 + 6 TM helices (Figure 1) (*7*−*10*).

MRP1 confers resistance to many commonly used, structurally diverse, natural product chemotherapeutic agents, including anthracyclines, epipodophylotoxins, and vinca alkaloids, as well as methotrexate and certain heavy metal oxyanions (*11*−*15*). Like P-gp, MRP1-mediated resistance is usually associated with an energy-dependent decrease in steady-state cellular accumulation of drugs as a consequence

† This work was supported by a grant from the National Cancer Institute of Canada with funds from the Terry Fox Run.

* To whom correspondence should be addressed. Tel.: (613) 533-2979. Fax: (613) 533-6830. E-mail: deeleyr@post.queensu.ca.

‡ Cancer Research Institute.

§ Current address: Eugene Mcdermott Center for Growth and Development, University of Texas Southwestern Medical Center at Dallas, 5323 Harry Hines Blvd., Dallas, TX 75390, USA.

⊥ Current address: Department of Xenobiotic Metabolism and Disposition, Minase Research Institute, Ono Pharmaceutical Co., Ltd, 3-1-1 Sakurai Shimamoto-cho, Mishima-gun, Osaka 618-8585, Japan.

Department of Anatomy and Cell Biology.

@ Department of Pathology and Molecular Medicine.

+ Canada Research Chair in Cancer Biology and Senior Scientist of Cancer Care Ontario

|| Department of Biochemistry.

[1] Abbreviations: MDR, multidrug resistance; MRP, multidrug resistance protein; P-gp, *P*-glycoprotein; CFTR, cystic fibrosis transmembrane conductance regulator; MSD, membrane-spanning domain; TM, transmembrane; NBD, nucleotide binding domain; ICD, intracellular domain; mAb, monoclonal antibody; $E_2$17βG, 17β-estradiol 17-(β-D-glucuronide); LTC_4, leukotriene C_4; MTT, 3-(4,5-dimethylthiazol-2-yl)-2,5-diphenyltetrazolium bromide; DOX, doxorubicin; VCR, vincristine; VP-16, etoposide; SDS−PAGE, sodium dodecyl sulfate−polyacrylamide gel electrophoresis; HEK, human embryonic kidney; PBS, phosphate-buffered saline.

10.1021/bi0495230 CCC: $27.50
Published on Web 07/02/2004

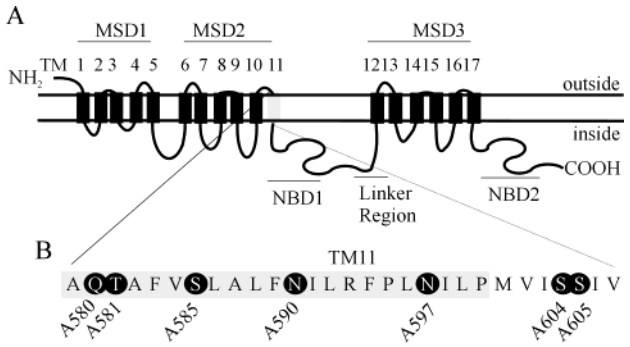

FIGURE 1: Topology of human MRP1. Panel A: the predicted topology of human MRP1 with 17 transmembrane (TM) helices. The putative TM11 is indicated by a lighter shading. Panel B: The amino acid sequence of MRP1 Ala^{579} to Val^{607} indicating polar amino acids subjected to mutation.

of increased drug efflux (*5*, *16*). However, considerable evidence indicates that MRP1 mediated transport of unmodified drugs, such as vincristine and doxorubicin, requires the presence of not only ATP but also reduced glutathione (GSH) (*17*−*21*). GSH appears to be cotransported with these unmodified drugs, although the stoichiometry of transport is not well-established (*20*−*22*).

In addition to conferring drug resistance, MRP1 transports a wide range of relatively hydrophilic glutathione-, glucuronate-, and sulfate-conjugated organic anions (*20*, *23*−*29*). Extensive in vitro transport studies using MRP1-enriched inside-out membrane vesicles have established that the protein is capable of direct, ATP-dependent transport of many organic anion conjugates, such as the glutathione conjugate cysteinyl leukotriene 4 (LTC_4) and the glucuronate conjugate 17β-estradiol 17-(β-D-glucuronide) ($E_2$17βG) (*20*, *23*−*25*). In contrast, MRP1-mediated transport of other organic anionic conjugates, such as the sulfate conjugate, estrogen-3-sulfate, and the glucuronate conjugate, 4-(methylnitrosamino)-1-(3-pyridyl)-1-butanol (NNAL)-*O*-glucuronide, is markedly stimulated by GSH (*28*, *29*). Unlike unmodified drugs such as vincristine and daunorubicin, neither estrogen-3-sulfate nor NNAL-*O*-glucuronide detectably stimulate GSH transport (*28*, *29*). What determines whether transport of a particular substrate is GSH dependent is not known.

How MRP1 binds and transports such a large number of structurally unrelated substrates remains an active area of study. We have shown that certain charged and polar aromatic amino acids, as well as a relatively large number of polar, nonaromatic amino acid residues appear to be important determinants of substrate specificity, suggesting that hydrogen bonding is an important contributor to substrate binding and possibly release (*30*−*33*, *50*). More recently, some amino acids predicted to be in extracellular or cytoplasmic regions have also been found to be important for the function of MRP1 (*34*, *35*).

In addition to the effects of mutations in various TM helices on substrate specificity, photoaffinity labeling studies of wild-type MRP1 with substrates and other ligands indicate that TMs10, -11 and -16, -17 may be major sites of cross-linking between bound ligand and protein (*36*−*39*). In ABC transporters with a more typical MSD structure, such as P-gp and CFTR, these helices correspond to TM's 5, 6 and 11, 12. In P-gp, TM6 has been shown to be particularly critical for substrate recognition (*40*, *41*). Mutational studies of CFTR have also demonstrated that certain residues, particularly polar residues such as Arg^{334}, Lys^{335}, Thr^{338}, Ser^{341}, and Arg^{347}, predicted to be located within TM6, are involved in forming the CFTR channel pore and determining the permeation properties of the protein (*42*−*44*). We have now investigated the role of polar residues within and near TM11 of MRP1 in determining the substrate specificity and/or overall activity of the protein. Amino acid residues Gln^{580}, Thr^{581}, Ser^{585}, Asn^{597}, and Ser^{605} were replaced individually by Ala. Ser^{604} was converted to Ala and Thr, and Asn^{590} was mutated to Ala, Gln, and Asp. These mutant proteins were then stably expressed in human embryonic kidney (HEK293) cells, and the transfectants were characterized with respect to their drug resistance profiles and ability to transport GSH, LTC_4, and $E_2$17βG. These studies demonstrate the importance of Asn^{597}, Ser^{604}, and Ser^{605} in defining the substrate specificity of MRP1 and of Asn^{590} in determining the overall activity of the protein. In addition, we show that the presence of an amino acid with side-chain hydrogen-bonding potential at position 590 in TM11 is required for efficient binding of ATP to NBD1 of the protein, thus providing a possible explanation for the pleiotropic effect of mutating this residue to nonpolar Ala.

EXPERIMENTAL PROCEDURES

Materials. Culture medium and fetal bovine serum were obtained from Life Technologies, Inc. [^{3}H]LTC_4 (38 Ci/mmol) and [^{3}H]GSH (52 Ci/mmol) were purchased from Amersham Pharmacia Biotech, [^{3}H]$E_2$17βG (44 Ci/mmol) from PerkinElmer Life Sciences, and 8-azido-[α^{32}P]ATP (11.8 Ci/mmol) from Affinity Labeling Technologies, Inc. (Lexington, KY). Doxorubicin HCl, etoposide (VP-16), and vincristine sulfate were obtained from Sigma.

Site-Directed Mutagenesis. Mutations Q580A, T581A, S604T, and S605A were generated using the Transformer-Site-Directed Mutagenesis kit (CLONTECH, Palo Alto, CA). Templates were prepared by cloning ~1.5−1.7 kilobase (kb) restriction fragments of MRP1 cDNAs into pGEM-3Zf (Promega). Mutagenesis was then performed according to the manufacturer's instructions using a selection primer 5′-GAG AGT GCA CGA TAT CCG GTG TG-3′ that mutates a unique NdeI site in the vector to an EcoRV restriction site. Oligonucleotides bearing mismatched bases at the residues to be mutated (underlined) were synthesized by ACGT Corp. (Toronto, Canada). They are as follows: Q580A (5′-C ATC CTG GAT GCC GCG ACG GCC TTC GTG TC-3′), T581A (5′-CTG GAT GCC CAG GCG GCC TTC GTG TCT TTG-3′), S605A (5′-C ATG GTC ATC AGC GCG ATC GTG CAG GCG-3′), and S604T (5′-CCC ATG GTC ATC ACT AGT ATC GTG CAG GCG-3′).

Mutations S585A, N590A, N590Q, N590D, N597A, and S604A were generated using the QuikchangeSite-Directed Mutagenesis kit (STRATAGENE, La Jolla, CA). Templates were prepared as described previously. Mutagenesis was then performed according to the manufacturer's instructions. Oligonucleotides bearing mismatched bases at the residues to be mutated (underlined) were synthesized by ACGT Corp. (Toronto, Canada). They are as follows: S585A (5′-C CAG ACA GCC TTC GTG GCT TTG GCC TTG-3), N590A (5′-CT TTG GCC TTG TTC GCC ATC CTC CGG TTT CCC-3′), N590Q (5′-CT TTG GCC TTG TTC CAG ATC CTC

CGG TTT CCC-3′), N590D (5′-CT TTG GCC TTG TTC GAT ATC CTC CGG TTT CCC-3′), N597A (5′-CTC CGG TTT CCC CTG GCC ATT CTC CCC ATG GT-3′), and S604A (5′-CTC CCC ATG GTC ATC GCC AGC ATC GTG CAG GC-3′)

After confirming all mutations by DNA Thermo Sequenase Cy5.5 and Cy5.0 dye terminator cycle sequencing (Amersham Biosciences) according to the manufacturer's instructions, DNA fragments containing the desired mutations were transferred into pCEBV7-MRP1. After the mutations were reconstructed into the full-length clones, the integrity of the entire mutated inserts and cloning sites was verified by DNA sequencing (ACGT Corp., Toronto, Canada).

Cell Lines and Tissue Culture. Stable transfection of HEK293 cells with the pCEBV7 vector containing the wild-type and mutant MRP1 cDNAs has been described previously (*14*, *30*, *31*, *45*). Briefly, HEK293 cells were transfected with pCEBV7 vectors containing mutant MRP1 using Fugene6 (Roche Molecular Biochemicals) according to the manufacturer's instructions. After ~48 h, the transfected cells were supplemented with fresh medium containing 100 μg/mL hygromycin B. Approximately 3 weeks after transfection, the hygromycin B-resistant cells were cloned by limiting dilution, and the resulting cell lines were tested for high-level expression of the mutant proteins.

Determination of Protein Levels in Transfected Cells. Plasma membrane vesicles were prepared by centrifugation through sucrose, as described previously (*14*, *19*). After determination of protein levels by Bradford assay (Bio-Rad), total membrane protein (0.5, 1.0, and 1.25 μg) from transfectants expressing wild-type MRP1 and various mutant proteins were analyzed by sodium dodecyl sulfate−polyacrylamide gel electrophoresis (SDS−PAGE) using a 7.5% gel. Proteins were subsequently transferred to Immobilon-P poly(vinylidene difluoride) membranes (Millipore, Bedford, MA) by electroblotting. The proteins were detected with mAb, MRPm6 (Alexis Biochemicals, San Diego, CA). Antibody binding was detected with horseradish peroxidase-conjugated goat anti-rat IgG (Pierce), followed by enhanced chemiluminescence detection and X-Omat Blue XB-1 films (PerkinElmer Life Sciences). Densitometry of the film images was performed using a ChemiImager 4000 (Alpha Innotech Corporation, San Leandro, CA). The relative protein expression levels were calculated by dividing the integrated densitometry values obtained for 0.5, 1.0, and 1.25 μg of total membrane proteins from transfectants expressing the mutant proteins by the integrated densitometry values obtained for the comparable amounts of total membrane proteins from transfectants expressing the wild-type protein. Each comparison was performed at least three times in independent experiments. The results were then pooled, and the mean values were used for normalization purposes.

Confocal Microscopy. Confocal microscopy was carried out as described previously (*30*, *31*, *45*). Briefly, ~5×10^5 stably transfected HEK293 cells were seeded in each well of a 6-well tissue culture dish on coverslips. When the cells had grown to confluence, they were washed once in phosphate-buffered saline (PBS) and then fixed with 2% paraformaldehyde in PBS, followed by permeabilization using digitonin (0.25 mg/mL in PBS). MRP1 proteins were detected with the monoclonal antibody MRPm6. Antibody binding was detected with Alexa Fluor 488 anti-mouse IgG (H + L) $(Fab')_2$ fragment. Nuclei were stained with propidium iodide. Localization of MRP1 in the transfected cells was determined using a Meridian Insight confocal microscope (filter, 620/40 nm for propidium iodide; 530/30 nm for Fluor 488).

Expression of the NH_2- and COOH-Proximal Half-Molecules of MRP1 in SF21 Cells. The construction of the dual expression vector pFASTBAC Dual (Life Technologies Inc.) encoding the NH_2- and the COOH-proximal half-molecules of MRP1 has been described previously (*46*). To generate the $MRP1^{N590A}$-pFASTBAC dual vector, pCEBV7-MRP1 containing mutation N590A was digested with BamHI and SphI, and an approximately 1.8 kb fragment comprised of nucleotides 840−2699 of $MRP1^{N590A}$ was isolated. This fragment was then ligated to an approximately 8.2 kb fragment isolated from BamHI and SphI digested MRP1-pFASTBAC dual vector.

Recombinant bacmids and baculoviruses were generated as described previously (*46*). The conditions used for viral infection were also similar to those described previously (*46*). Plasma membrane vesicles were prepared, and the expression levels of wild-type and mutant protein in infected cells were determined, as described previously. The NH_2-proximal proteins were detected with mAb, MRPr1 (Alexis Biochemicals, San Diego, CA), and the COOH-proximal proteins were detected with mAb, MRPm6 (Alexis Biochemicals, San Diego, CA).

LTC_4, $E_2$17βG, and GSH Transport by Membrane Vesicles. Plasma membrane vesicles were prepared as described previously, and ATP-dependent transport of [^{3}H]LTC_4 into the inside-out membrane vesicles was measured by a rapid filtration technique (*19*, *23*, *47*). Briefly, vesicles (10 μg of total proteins) were incubated at 23 °C in 100 μL of transport buffer (50 mM Tris-HCl, 250 mM sucrose, 0.02% sodium azide, pH 7.4) containing ATP or AMP (4 mM), 10 mM $MgCl_2$, and [^{3}H]LTC_4 (50 nM, 200 nCi). At the indicated times, 20 μL aliquots were removed and added to 1 mL of ice-cold transport buffer, followed by filtration under vacuum through glass fiber filters (type A/E, Gelman Sciences, Dorval, Quebec, Canada). Filters were immediately washed twice with 4 mL of cold transport buffer. The bound radioactivity was determined by scintillation counting. All data were corrected for the amount of [^{3}H]LTC_4 that remained bound to the filter in the absence of vesicle protein (usually <5% of the total radioactivity). [^{3}H]LTC_4 uptake was expressed relative to the total protein concentration in each reaction. ATP-dependent uptake of [^{3}H]$E_2$17βG (400 nM, 120 nCi) was measured as described for [^{3}H]LTC_4 except that the reaction was carried out at 37 °C.

K_m and V_{max} values of ATP-dependent [^{3}H]LTC_4 uptake by membrane vesicles (2.5 μg of total proteins) were measured at various LTC_4 concentrations (0.01−1 μM) for 1 min at 23 °C in 25 μL of transport buffer containing 4 mM ATP and 10 mM $MgCl_2$, followed by nonlinear regression analyses. Kinetic parameters of ATP-dependent [^{3}H]$E_2$17βG (0.1−16 μM) uptake were determined as described for [^{3}H]LTC_4 except that the reaction was carried out at 37 °C.

GSH uptake was also measured by rapid filtration with membrane vesicles (20 μg of total proteins) incubated at 37 °C for 20 min in a 60 μL reaction volume with [^{3}H]GSH (100 μM, 300 nCi). To minimize GSH catabolism by

γ-glutamyltranspeptidase during transport, membranes were preincubated in 0.5 mM acivicin for 10 min at 37 °C prior to measuring [^{3}H]GSH uptake in the presence of verapamil (100 μM).

Photoaffinity Labeling of the Wild-Type and Mutant Proteins with [^{3}H]LTC$_4$. Wild-type and mutant MRP1 membrane proteins were photolabeled with [^{3}H]LTC$_4$ essentially as described previously (*19*, *36*). Briefly, membrane vesicles (50 μg of total proteins in 35 μL of transport buffer) were incubated with [^{3}H]LTC$_4$ (0.3 μCi, 200 nM) at room temperature for 30 min, frozen in liquid nitrogen, and UV-irradiated. Proteins were analyzed on a 5−15% gradient gel by SDS−PAGE. The gel was then fixed treated with Amplify (Amersham Biosciences), dried, and exposed to film for 1 week at −70 °C.

Chemosensitivity Testing. Drug resistance was determined using the colorimetric 3-(4,5-dimethylthiazol-2-yl)-2,5-diphenyl tetrazolium bromide (MTT) assay as described previously (*11*, *12*, *14*). Mean values of quadruplicate determinations (×b1SD) were plotted using GraphPad software. IC$_{50}$ values were obtained from the best fit of the data to a sigmoidal curve. Relative resistance is expressed as the ratio of the IC$_{50}$ value of cells transfected with MRP1 expression vectors as compared with cells transfected with empty vector. Resistance was determined in three or more independent experiments.

Photolabeling of MRP1 with 8-Azido-[α^{32}P]ATP and Orthovanadate-Induced Trapping of 8-Azido-[α^{32}P]ATP by MRP1. Wild-type and mutant MRP1 membrane proteins were photolabeled with 8-azido-[α^{32}P]ATP essentially as described previously (*46*). Briefly, membrane vesicles (20 μg of total proteins in 10 μL of transport buffer containing 5 mM $MgCl_2$) were incubated with 8-azido-[α^{32}P]ATP (1 μCi) on ice for 5 min and UV-irradiated. The reactions were stopped by the addition of 400 μL of ice-cold stop buffer (50 mM Tris-Cl, pH 7.2, 0.1 mM EGTA, 5 mM $MgCl_2$), and the membranes were centrifuged at 14 000 rpm for 15 min at 4 °C. The pellets were resuspended in 20 μL of stop buffer and were then analyzed on a 5−15% gradient gel by SDS−PAGE. The gel was then dried and exposed to film for 2 h at room temperature.

Orthovanadate-induced trapping of 8-azido-[α^{32}P]ATP by MRP1 was determined as described previously (*46*). Briefly, membrane proteins (20 μg of total proteins) were incubated in transport buffer (10 μL) containing 5 mM $MgCl_2$, 1 mM sodium orthovanadate, and 8-azido-[α^{32}P]ATP (1 μCi) in the presence and absence of 1 μM LTC$_4$ at 37 °C for 15 min. The reactions were stopped by the addition of 400 μL of ice-cold stop buffer, and the membranes were centrifuged at 14 000 rpm for 15 min at 4 °C. The pellets were washed again and resuspended in 20 μL of stop buffer. The samples were transferred to a 96-well plate and UV-irradiated. Proteins were analyzed on a 5−15% gradient gel by SDS−PAGE. The gel was then dried and exposed to film for 6 h at room temperature.

RESULTS

Expression of Mutant MRP1 in Stably Transfected HEK293 Cells. We have previously shown that mutations of amino acid residues with side-chain hydrogen-bonding potential in several TM helices in MRP1 can drastically affect the substrate specificity of the protein (*30*−*32*). The most extensively analyzed helix to date is TM17, which photoaffinity labeling studies indicate may be a major site of cross-linking between bound ligand and protein. Such studies have also implicated TM11 as part of a major drug-binding site (*36*, *39*). Most recently, a possible MRP1 structure, based on homology modeling with a predicted structure of P-gp and the crystal structure of VC-MsbA, led to the identification of a Phe residue (Phe^{594}) in TM11 that was important for the overall activity of the protein. Nonconservative mutation of Phe^{594} to Ala resulted in decreased transport of all substrates tested and loss of photolabeling with LTC$_4$. In contrast, conservative mutation to Tyr and Trp resulted in residue-dependent changes in substrate specificity (*48*). Like the F594A mutation, nonconservative substitution of the two adjacent residues Arg^{593} and Pro^{595} also decreased transport of all organic anion substrates tested (*35*, *49*). TM 11 of MRP1 contains a relatively high proportion of polar residues. To examine their possible importance in determining the overall activity and substrate specificity of MRP1, we generated a series of seven mutant proteins in which Gln^{580}, Thr^{581}, Ser^{585}, Asn^{597}, Ser^{604}, Ser^{605}, and Asn^{590} were replaced individually by Ala (Figure 1).

The episomal expression vector, pCEBV7, containing mutated forms of MRP1 cDNAs was used to stably transfect HEK293 cells, and populations of transfected cells were selected in hygromycin B. The resultant stably transfected cell populations were cloned by limiting dilution, and subpopulations expressing high levels of MRP1 mutant proteins were used in subsequent studies. The levels of mutant proteins relative to wild-type MRP1 in previously characterized HEK transfectants were determined by immunoblotting and densitometry (Figure 2A). Endogenous MRP1 in HEK293 cells transfected with the empty vector was undetectable under the conditions used (data not shown). The expression levels of seven of the mutant proteins in stably transfected HEK293 cells were similar to that of wild-type MRP1.

To determine whether these mutations influenced trafficking of the protein, we compared the subcellular localization of wild-type and mutant MRP1 by confocal microscopy. As shown in Figure 2B, the subcellular distribution of the mutated proteins assessed by immunoreactivity with the MRP1 specific mAb MRPm6 was indistinguishable from that of cells expressing wild-type protein. In all cases, strong plasma membrane staining was observed, indicating that trafficking was unaffected.

Transport of [^{3}H]LTC$_4$ and [^{3}H]E$_2$17βG by Wild-Type and Mutant MRP1. To determine whether any of the mutations altered the efficiency with which the protein transported LTC$_4$ and E$_2$17βG, we examined ATP-dependent uptake of these compounds by membrane vesicles prepared from HEK transfectants expressing each of these mutant proteins (Figure 3). The levels of LTC$_4$ uptake by vesicles prepared from HEK transfectants expressing either wild-type MRP1 or mutations Q580A, T581A, S585A, N597A, S604A, and S605A were proportional to the relative expression levels of the wild-type and mutant proteins. The only mutation that affected LTC$_4$ transport was replacement of Asn^{590} by Ala, which decreased the ability of MRP1 to transport LTC$_4$ by approximately 50−60% (Figure 3A−D).

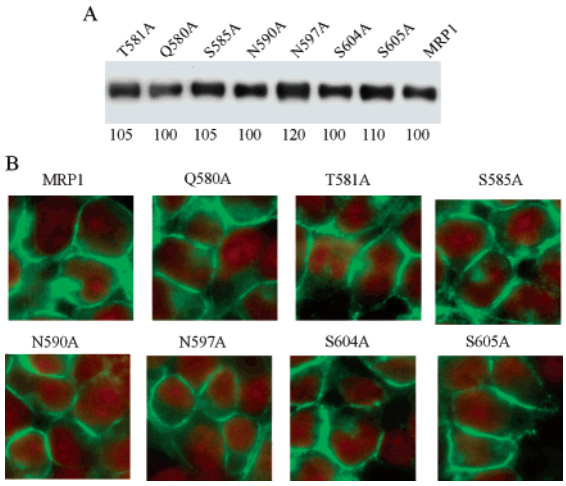

FIGURE 2: Expression of mutant MRP1 in stably transfected HEK293 cells. Panel A: expression levels of wild-type and mutant MRP1 proteins in membrane vesicles isolated from stably transfected HEK293 cells were determined by immunobloting of membrane vesicle preparations and densitometry as described. Blots were probed with the MRP1-specific mAb MRPm6. The numbers below the blot refer to the levels of the mutant MRP1 proteins relative to the levels of wild-type MRP1 proteins in membrane vesicles prepared from the stably transfected HEK293 cells. Similar results were obtained from eight more experiments. Panel B: subcellular localization of wild-type and mutant MRP1 was determined by confocal microscopy as described. MRP1 was detected using mAb MRPm6. Location of MRP1 is indicated in green. Nuclei were stained with propidium iodide and are shown in red. Transfectants tested were expressing wild-type or mutant MRP1 as indicated in the figure. An $x-y$ optical section of the cells is shown to illustrate the distribution of the wild-type and mutant proteins between plasma and intracellular membranes.

ATP-dependent transport of [^{3}H]E$_2$17βG was also examined (Figure 3E−H). Mutations Q580A, T581A, S585A, N597A, and S605A had no detectable effect on transport. However, substitution of Ser^{604} with Ala (S604A) increased the transport efficiency by approximately 2-fold. On the other hand, replacement of Asn^{590} with Ala (N590A) substantially decreased the levels of E$_2$17βG transport. Thus, mutation S604A altered only the ability of MRP1 to transport the glucuronidated estrogen, whereas mutation N590A influenced the transport of both LTC$_4$ and E$_2$17βG.

Effect of Mutations S604T, N590Q, and N590D on Transport of [^{3}H]LTC$_4$ and [^{3}H]E$_2$17βG by Wild-Type MRP1. Replacement of Ser^{604} and Asn^{590} with nonpolar Ala increased the levels of E$_2$17βG transport or decreased the transport of both LTC$_4$ and E$_2$17βG, respectively. Consequently, we examined the effect of more conservative substitution of these residues with other polar amino acids. Ser^{604} was mutated to Thr, and Asn^{590} was converted to Asp and Gln. The mutant proteins were then stably expressed in HEK293 cells. Their expression levels were similar to that of wild-type MRP1 (Figure 4A). The effects of all of the mutations on the ability of MRP1 to transport LTC$_4$ and E$_2$17βG are shown in Figure 4B,C. Mutations N590Q, N590D, and S604T had no effect on transport of the two substrates. These results suggest that the polar character of the residue side chain at positions 590 and 604 but not their size is important in defining the efficiency with which wild-type MRP1 transports both LTC$_4$ and E$_2$17βG.

Kinetic Parameters of [^{3}H]LTC$_4$ and [^{3}H]E$_2$17βG Transport by Wild-Type and Mutant MRP1. To examine the influence of the N590A and S604A mutations more quantitatively, we compared their effect on the kinetic parameters of transport of both substrates (Figure 5). Mutation S604A had no effect on either the apparent K_m or V_{max} values for LTC$_4$ uptake (K_m 150 and 145 nM, and V_{max} 89 and 84 pmol/mg/min for wild-type MRP1 and mutation S604A, respectively) (Figure 5B and Table 1). In contrast, the N590A mutation decreased the V_{max} and increased the apparent K_m value for LTC$_4$ transport (56 pmol/mg/min and 277 nM for mutation N590A) (Figure 5B and Table 1). Thus, mutation N590A decreased the V_{max}/K_m ratio for LTC$_4$ approximately 3-fold.

Table 1: Kinetic Parameters of LTC$_4$ and E$_2$17βG Uptake by Vesicles from HEK Cells Transfected with Vectors Encoding Wild-Type and Mutant Proteins[a]

	K_m (μM)		V_{max} (pmol/ mg/min)		V_{max}/K_m	
transfectant	LTC$_4$	E$_2$17βG	LTC$_4$	E$_2$17βG	LTC$_4$	E$_2$17βG
HEK$_{MRP1}$	0.150	1.7	89	197	593	116
HEK$_{MRP1N590A}$	0.277	2.8	56	93	202	33
HEK$_{MRP1S604A}$	0.145	0.7	84	241	579	344

[a] The kinetic parameters of LTC$_4$ and E$_2$17βG uptake were determined as described in the legend to Figure 5.

For E$_2$17βG transport, the V_{max} value for mutation S604A was increased by 20−25% relative to wild-type MRP1 (197 pmol/mg/min for wild-type MRP1 vs 241 pmol/mg/min for the mutation), while the apparent K_m was decreased ~2.5-fold (1.7 and 0.7 μM for wild-type MRP1 and mutation S604A, respectively) (Figure 5C and Table 1). In contrast, substitution of Asn^{590} with Ala increased the K_m value by approximately 65% (2.8 μM) and decreased the V_{max} value by approximately 2-fold (93 pmol/mg/min) (Figure 5C and Table 1). Thus, as observed with LTC$_4$ as a substrate, mutation N590A decreased the V_{max}/K_m ratio for E$_2$17βG approximately 3-fold, whereas the S604A mutation increased the V_{max}/K_m ratio for this substrate approximately 3-fold. These changes in transport efficiency were mediated predominantly by a decrease in apparent affinity for both LTC$_4$ and E$_2$17βG as a result of the S604A mutation, while the N590A mutation increased the apparent K_m and decreased the V_{max} for E$_2$17βG.

Photolabeling of the Wild-Type and Mutant Proteins with [^{3}H]LTC$_4$. Since transport studies indicated that mutation N590A increased the apparent K_m for LTC$_4$, we directly examined the ability of the mutant protein to bind and be photolabeled by [^{3}H]LTC$_4$. The N590A mutation decreased photolabeling, consistent with the results obtained with kinetic analysis of LTC$_4$ uptake (Figure 6B). We have shown previously that a decrease in affinity for substrate occurs when NBD2 is occupied by either ATP or ADP. Although photolabeling of the N590A mutant protein was decreased relative to wild type in the absence of ATP, a further decrease was observed in the presence of nucleotide, indicating that the protein retains the ability to shift from a higher to lower affinity state. To investigate the effect of mutation N590A on photolabeling of LTC$_4$ more precisely, we took advantage of a pFASTBAC dual vector, in which the NH$_2$-proximal MRP1 fragment (amino acids 1−932) was modified to contain mutation N590A and coexpressed with a wild-type COOH-proximal fragment (amino acids 932−1531). The wild-type and mutant MRP1-pFASTBAC dual vectors were

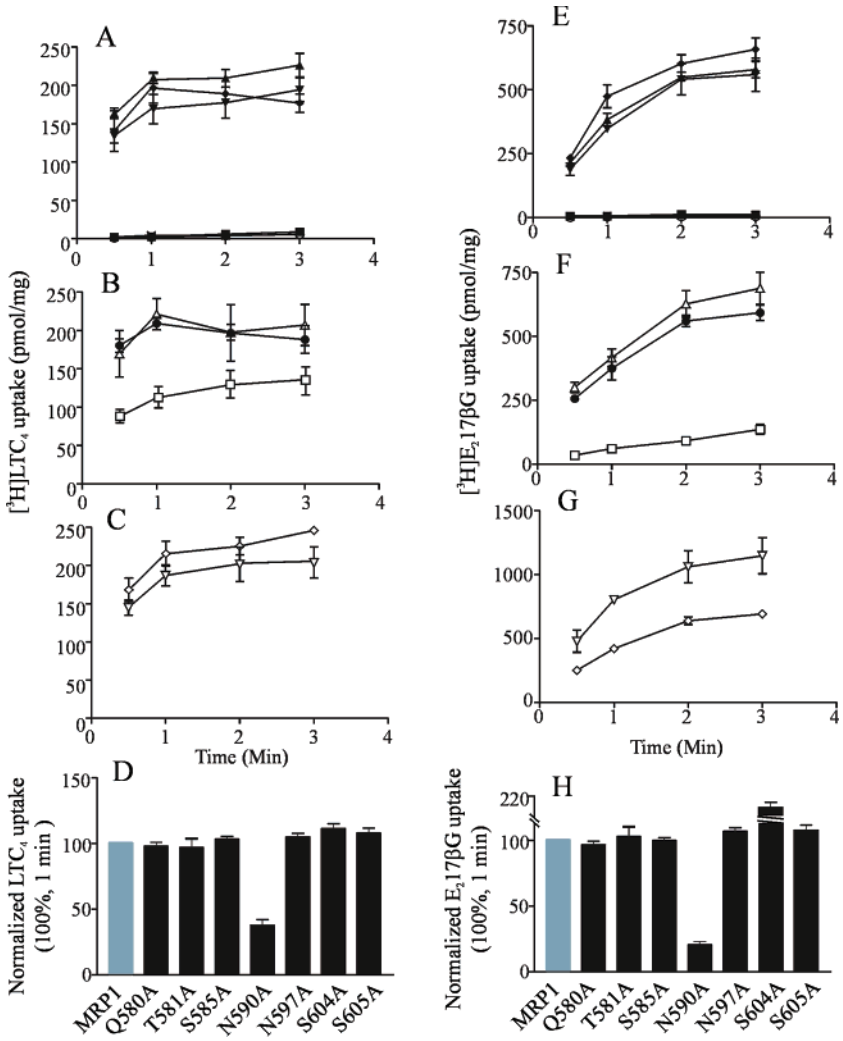

FIGURE 3: ATP-dependent [^{3}H]LTC$_4$ and [^{3}H]E$_2$17βG uptake by membrane vesicles prepared from HEK293 cells stably transfected with wild type or mutant MRP1. Panels A−D: LTC$_4$ uptake. Membrane vesicles were incubated at 23 °C with 50 nM LTC$_4$ (200 nCi) in transport buffer for the time indicated, as described. Panel E−H: ATP-dependent uptake of [^{3}H]E$_2$17βG (400 nM, 120 nCi) was measured as described for [^{3}H]LTC$_4$ except that the reaction was carried out at 37 °C. Transfectants tested were HEKpc$_7$(■), HEK$_{MRP1}$(▲), HEK$_{MRP1Q580A}$-(▼), HEK$_{MRP1T581A}$(◆), HEK$_{MRP1S585A}$(●), HEK$_{MRP1N590A}$(□), HEK$_{MRP1N597A}$(△), HEK$_{MRP1S604A}$(▽), and HEK$_{MRPS605A}$(◇). The uptake of LTC$_4$ and E$_2$17βG by membrane vesicles prepared from control and wild-type MRP1-transfected HEK293 cells in transport buffer containing 4 mM AMP was also examined and shown in panels A and D [HEKpc$_7$(○), and HEK$_{MRP1}$(+)]. The normalized transport values were obtained by adjusting experimentally determined values (1 min time point) to compensate for differences in the relative levels of the wild-type and mutant proteins and are shown in panels D and H as gray bars. Data shown in panels A−F have not been normalized to compensate for differences in expression levels. Values are mean ± SD of ≥3 independent experiments.

then used to infect SF21 cells. The expression levels of both NH_2- and COOH-proximal fragments encoded by the mutant MRP1^{N590A} pFASTBACK dual vector were slightly lower that those of the wild-type half-molecules (Figure 6C). The ATP-dependent LTC$_4$ uptake by reconstituted mutant and wild-type proteins was then determined by transport assays (Figure 6D). As observed with results obtained from analyses of membrane vesicles prepared from HEK293 cells stably transfected with full-length mutant MRP1^{N590A}, replacement of Asn^{590} by Ala decreased the transport activity by approximately 50%. Photolabeling of mutant dual-half proteins with [^{3}H]LTC$_4$ was then carried out. As shown in Figure 6E, the N590A mutation resulted in a significant reduction of the labeling of LTC$_4$ at both the NH_2- and the COOH-proximal halves of MRP1. In addition, we observed that ATP could significantly decrease the labeling of the NH_2-proximal half of wild-type MRP1, consistent with previous studies (*46*).

Resistance Profiles of Wild-Type and Mutant Human Proteins. The drug resistance profiles of transfectants expressing mutant proteins were also determined using MTT assays. The results are presented as relative drug resistance factors in Table 2. Mutations Q580A, T581A, S585A, S604A, and S604T had no significant effect on the ability of MRP1 to confer resistance to any drug tested. In contrast, conversion of Asn^{597} to Ala resulted in a mutant protein with enhanced resistance to vincristine (3−4-fold) but an approximately 3-fold decrease in the ability to confer resistance to VP-16 without any significant effect on doxorubicin resistance. On the other hand, despite the fact that converting Asn^{590} to either Gln or Asp had no effect on the drug resistance profile of MRP1, substitution of the residue with Ala significantly decreased resistance to vincristine, doxorubicin, and VP-16. Replacement of Ser^{605} by Ala also resulted in approximately a 2−3-fold reduction of resistance to all three drugs tested. Thus, Asn^{597} affects the drug

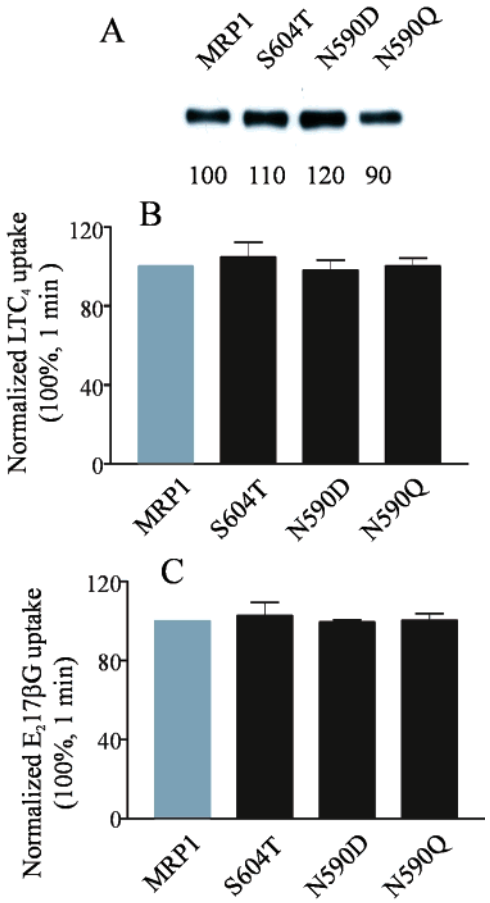

FIGURE 4: ATP-dependent [^{3}H]LTC$_4$ and [^{3}H]E$_2$17βG uptake by membrane vesicles prepared from HEK293 cells transfected with wild-type or mutant MRP1. Panel A: expression levels of wild-type and mutant MRP1 proteins in membrane vesicles isolated from stably transfected HEK293 cells were determined by immunobloting of membrane vesicle preparations and densitometry as described in the legend to Figure 2A. [^{3}H]LTC$_4$ (B) and [^{3}H]E$_2$17βG (C) uptake by wild-type and mutant proteins was determined as described in the legend to Figure 3. The normalized transport values were obtained by adjusting experimentally determined values (1 min time point) to compensate for differences in the relative levels of the wild-type and mutant proteins. Values are mean ± SD of ≥3 independent experiments.

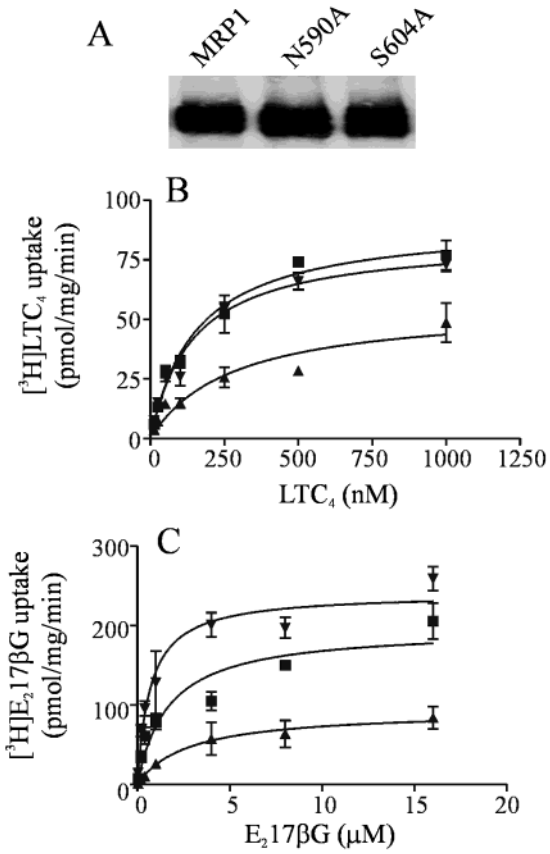

FIGURE 5: Kinetics of ATP-dependent [^{3}H]LTC$_4$ and [^{3}H]E$_2$17βG uptake. Panel A: Expression levels of wild-type and mutant MRP1 proteins in membrane vesicles isolated from transiently transfected HEK293 cells were determined by immunobloting of membrane vesicle preparations and densitometry as described in the legend to Figure 2A. The expression levels of the mutant proteins were similar to that of wild-type MRP1. Panel B: The initial rate of ATP-dependent [^{3}H]LTC$_4$ uptake by membrane vesicles prepared from HEK293 cells transfected with wild-type or mutant proteins was measured at various LTC$_4$ concentrations (0.01−1 μM) for 1 min at 23 °C as described. Panel C: [^{3}H]E$_2$17βG uptake was determined as described for [^{3}H]LTC$_4$ except that the reactions were carried out at 37 °C with various concentrations of E$_2$17βG (0.1−16 μM). Values are mean ± SD of triplicate determinations in a single experiment. Similar results were obtained from two more experiments. Data were plotted as V_0 vs [S] to confirm that the concentration range selected was appropriate to observe both zero- and first-order rate kinetics. The transfectants tested were HEK$_{MRP1}$(■), HEK$_{MRP1N590A}$(▲), and HEK$_{MRP1S604A}$(▼). Kinetics parameters for LTC$_4$ and E$_2$17βG transport were determined from nonlinear regression analysis of the combined data and are shown in Table 1.

specificity of MRP1, while Asn^{590} and Ser^{605} influence the level of resistance to all three classes of drugs tested.

Transport of [^{3}H]GSH by Wild-Type and Mutant MRP1. The studies described previously showed that the N590A mutation modulated the ability of MRP1 to confer drug resistance and to transport conjugated organic anions. In contrast, mutations N597A and S605A influenced only the drug resistance profile of MRP1, and mutation S604A affected the transport of only E$_2$17βG. One major distinction between MRP1-mediated transport of conjugated substrates, such as LTC$_4$ and E$_2$17βG, and drugs, such as vincristine and daunorubicin, is a requirement for GSH (*17*−*20*), which may be cotransported with the unmodified drug. This suggested that the mutations might have affected the interaction of GSH with the protein (*19*, *22*). To examine this possibility, we took advantage of our previous demonstration that MRP1 exhibits low levels of ATP-dependent GSH transport in the absence of a second substrate and that GSH transport can be dramatically stimulated by verapamil (*51*). As observed with the effects of the mutations on LTC$_4$ transport, only replacement of Asn^{590} with Ala significantly decreased the ability of MRP1 to transport GSH (Figure 7). Other mutations, including N597A and S605A, which influenced MRP1-mediated drug resistance, had no effect, suggesting that they modify interactions between MRP1 and the drug rather than altering the ability to bind and transport GSH.

Effect of Mutation N590A on Photolabeling of MRP1 with 8-Azido-[α^{32}P]ATP. On the basis of all substrates tested, mutation N590A affected the overall activity of MRP1. Most recently, we reported that conversion of Asp^{1084}, predicted to be at/ near the cytoplasm/membrane interface of TM14, both decreased the overall transport activity of MRP1 and markedly reduced the hydrolysis of ATP at NBD2 of MRP1 (*33*). To investigate whether the N590A mutation influenced the binding and/or hydrolysis of ATP at NBD1 and/or NBD2

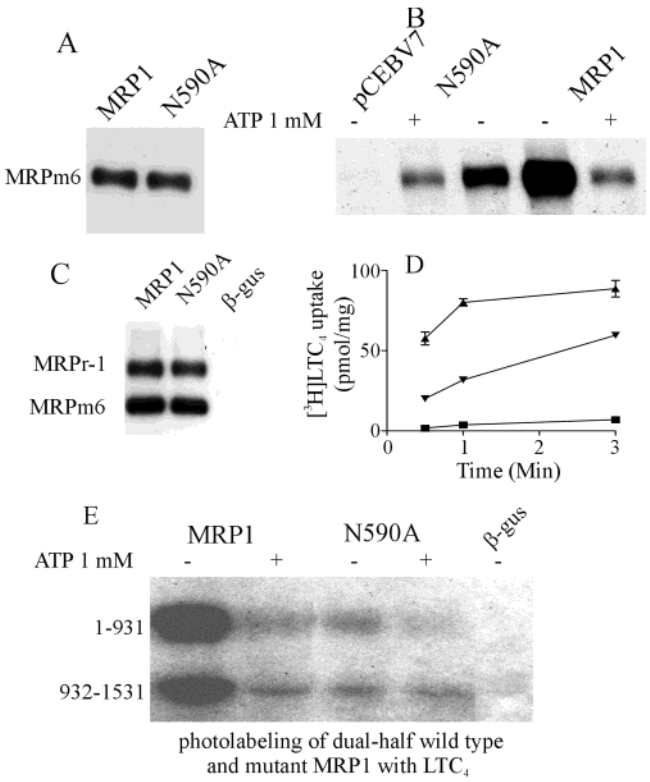

FIGURE 6: Photolabeling of wild-type and mutant MRP1 with [^{3}H]-LTC_4. Panel A: expression levels of wild-type and mutant MRP1 proteins in membrane vesicles isolated from stably transfected HEK293 cells used for photolabeling experiments were determined by immunobloting of membrane vesicle preparations and densitometry as described in the legend to Figure 2A. Panel B: [^{3}H]LTC_4 photolabeling was determined as described. Membrane vesicles (40 μg of total proteins in 40 μL of transport buffer) were incubated with [^{3}H]LTC_4 (0.3 μCi, 200 nM) at room temperature for 30 min in the presence and absence of ATP (1 mM), following the binding procedure as described. Similar results were obtained from three more experiments. Panel C: Expression levels of the wild-type and mutant dual-half MRP1 proteins in membrane vesicles prepared from infected SF21 cells were determined by immunobloting and densitometry as described. Panel D: [^{3}H]LTC_4 uptake by the wild-type and mutant dual-half proteins was determined as described in the legend to Figure 3. Transfectants tested were β-gus(■), MRP1-dual half (▲), and $MRP1^{N590A}$-dual half(▼). Panel E: Photolabeling of the wild-type and mutant dual-half proteins with [^{3}H]LTC_4 was determined as described. Similar results were obtained from three more experiments.

of MRP1, we used the baculovirus dual expression system to examine the effect of the mutation on photolabeling of MRP1 by 8-azido-[α^{32}P]ATP. The protein was photolabeled at both 4 °C to minimize hydrolysis of the 8-azido-[α^{32}P]-ATP and 37 °C in the presence of vanadate to trap 8-azido-[α^{32}P]ADP. We and others have shown previously that, at 4°C, ATP binds primarily to NBD1 while under trapping conditions, the majority of ADP is found associated with NBD2 (*46*, *52*). As shown in Figure 8B, substitution of Asn^{590} with Ala dramatically decreased the binding of the ATP analogue at NBD1. Binding was also decreased at NBD2, which is consistent with previous observations that binding of ATP to NBD1 is a prerequisite for efficient binding at NBD2 (*46*, *59*). In contrast, the mutation only modestly decreased vanadate-dependent trapping of 8-azido-[α^{32}P]ADP by NBD2 (Figure 8C).

Previously, we have shown that the vanadate-dependent trapping of 8-azido-[α^{32}P]ADP predominantly by NBD2 of MRP1 was enhanced in the presence of LTC_4, consistent with a substrate dependent stimulation of ATP hydrolysis at NBD2 (*46*). Consequently, we investigated the possibility that the general decrease in transport activity of the protein might be attributable to loss of substrate-dependent stimulation of the basal ATPase activity of the protein. However, as shown in Figure 8C, no significant difference could be detected between wild-type and N590A mutant proteins with respect to the ability of the LTC_4 to enhance ADP trapping at NBD2 (compare lanes 5 and 6 and lanes 2 and 3 in Figure 8C) (*46*).

DISCUSSION

Photolabeling studies have implicated TM11 of MRP1 in substrate binding, and we have shown previously that nonconservative substitution of any of three amino acids predicted to be near the middle of the helix causes an overall decrease in transport activity (*35*, *48*, *49*). To further define the role of amino acids in TM11 in determining substrate specificity and overall activity, we have extended our mutational studies to seven previously uninvestigated polar residues that span from the cytoplasmic to extracellular interfaces of the helix. On the basis of the substrates tested, we found that mutations of three polar residues Gln^{580}, Thr^{581}, and Ser^{585}, predicted to be in the outer leaflet region of TM11 and the immediately adjacent segment of the extracellular loop, had no detectable effect on protein function. On the other hand, Ala substitution of three polar residues, Asn^{597}, Ser^{604}, and Ser^{605}, predicted to be in the inner leaflet of the membrane and near the cytoplasmic/ membrane interface, clearly influenced substrate specificity (Figure 9). In contrast, rather than altering substrate specificity, replacement of Asn^{590} with Ala uniformly decreased the overall activity of MRP1, both with respect to transport of organic anion conjugates and resistance to three different classes of drugs. Thus, the consequences of the N590A mutation are similar to those of nonconservative mutations of other amino acids (Arg^{593}, Phe^{594}, and Pro^{595}) predicted to be near the middle of TM11 (*35*, *48*, *49*).

Studies of the distantly related bacterial drug transporter, LmrA, suggest that TM6 of the protein, which as in the case of P-gp and CFTR corresponds topologically to TM11 of MRP1, has one face of the helix exposed to an aqueous cavity that might form a pathway through which substrates cross the membrane (*53*). Similarly, studies of CFTR indicate a number of residues in TM 6 have side chains that are accessible from the aqueous pore of the channel and that are important for anion binding, as well as in some cases, anion selectivity (*42*−*44*). These residues tend to cluster in the middle section of the predicted helix, similar to the cluster of Asn^{590} to Pro^{595} in TM11 of MRP1 (*43*). In P-gp, residues in TM6 that have been implicated in the binding of verapamil and certain derivatives are located predominantly in the cytoplasmic proximal half of the helix and thus also align closely with those we have identified in the inner leaflet region of TM11 (*40*). Examination of the predicted three-dimensional structures for TM11 of MRP1 indicates that all mutation-sensitive polar residues (Asn590, Arg593, Asn597, Ser604, Ser605) and the mutation-sensitive Phe^{594} are located within an approximate 90° arc on one side of the helix (Figure 9) (*48*). Consequently, depending on the rotational orientation of the helix, these residues could be exposed to

Table 2: Relative Drug Resistance of HEK293 Cells Transfected with Wild-Type and Mutant MRP1[a]

transfectant	drug (relative resistance factor)		
	vincristine	VP-16	doxorubicin
HEK_{MRP1}	36.0 ± 7.5 (36.0)	12.5 ± 2.7 (12.5)	9.6 ± 0.9 (9.6)
$HEK_{MRP1Q580A}$	32.5 ± 7.8 (32.5)	10.6 ± 1.1 (10.7)	11.7 ± 2.8 (11.7)
$HEK_{MRP1T581A}$	41.2 ± 8.8 (39.2)	14.6 ± 2.7 (13.9)	12.1 ± 0.9 (11.1)
$HEK_{MRP1S585A}$	37.6 ± 7.7 (35.8)	12.7 ± 2.4 (12.1)	9.4 ± 0.9 (9.0)
$HEK_{MRP1N590A}$	10.5 ± 2.9 (10.5)	2.4 ± 0.6 (2.4)	2.7 ± 0.7 (2.7)
$HEK_{MRP1N590Q}$	28.9 ± 6.0 (32.1)	9.5 ± 2.0 (10.5)	10.5 ± 3.8 (11.6)
$HEK_{MRP1N590D}$	38.9 ± 2.3 (32.4)	13.6 ± 0.2 (11.3)	10.2 ± 2.2 (8.5)
$HEK_{MRP1N597A}$	131.2 ± 27.1 (109.3)	6.8 ± 2.8 (5.7)	10.4 ± 4.5 (8.7)
$HEK_{MRP1S604A}$	38.0 ± 8.6 (38.0)	12.1 ± 5.6 (12.1)	10.6 ± 1.7 (10.6)
$HEK_{MRP1S604T}$	36.9 ± 6.6 (33.5)	12.1 ± 0.6 (11.0)	8.9 ± 1.5 (8.1)
$HEK_{MRP1S605A}$	12.4 ± 2.2 (11.3)	7.8 ± 0.1 (7.1)	3.8 ± 0.2 (3.5)

[a] The resistance of HEK293 cells transfected with expression vectors encoding wild-type and mutant MRP1 relative to that of cells transfected with empty vector were determined using a tetrazolium salt-based microtiter plate assay. The relative resistance factor was obtained by dividing the IC_{50} values for wild-type/mutant MRP1-transfected cells by the IC_{50} value for control transfectants. The values shown represent the mean standard deviation (±SD) of relative resistance values determined from three independent experiments. Resistance factors normalized for differences in the levels of mutant proteins expressed in the transfectant populations used are shown in parentheses.

an aqueous pore serving as a pathway through the membrane for MRP1 substrates. The exception is Pro^{595}, which is predicted to cause a kink in the backbone of TM11 and is oriented toward the opposite side of the helix from the other residues. Neither P-gp nor CFTR contain a comparable Pro residue in TM6. It appears likely that mutation of Pro^{595} would perturb the relative positions of a number of other critical residues in TM11 that may account, at least in part, for its effect on the overall activity of the protein (*35*).

How each residue interacts with different substrates is not yet known. Previous studies in MRP1, MRP3, and P-gp suggest that the size of amino acid side chain affects substrate specificity with small side chains favoring interaction with larger substrates (*30*, *33*, *54*, *55*). Consistently, we found that replacement of Asn^{597} with Ala increased resistance to larger drugs such as vincristine and decreased resistance to smaller substrates such as VP-16. In addition, although mutation S604T had no effect on any of the MRP1 functions tested, converting Ser^{604} to Ala decreased the apparent K_m values and increased V_{max} for $E_2 17\beta G$ uptake. These findings suggest that elimination of the polar character of the residue side chain at position 604 may facilitate the interaction of the protein with the conjugated estrogen, thereby enhancing transport activity. On the other hand, mutation of Ser^{605} to Ala decreased the ability of MRP1 to confer resistance to vincristine, VP-16, and doxorubicin, consistent with our previous proposal that hydrogen bonding may be a common form of interaction between MRP1 and its substrates (*30*−*33*, *45*, *55*, *60*). In addition, mutations N597A and S605A affected only the drug-resistance profile of MRP1. Since at least some unmodified drugs are cotransported by MRP1 together with GSH, this observation raised the possibility that Asn^{597} and Ser^{605} residues might be involved in the cotransport mechanism (*19*, *22*). However, the two mutations had no effect on the verapamil-stimulated transport of GSH, suggesting that they are more likely to participate in the interaction of MRP1 with the drug substrate rather than GSH.

The conversion of Asn^{590} to Ala substantially decreased the ability to confer drug resistance and to transport $E_2 17\beta G$, LTC_4, and GSH. It also decreased the binding of LTC_4, as assessed by photolabeling experiments. Consistent with requirement for a hydrogen-bonding side chain at this location, mutation to either Asp or Gln had no effect on any

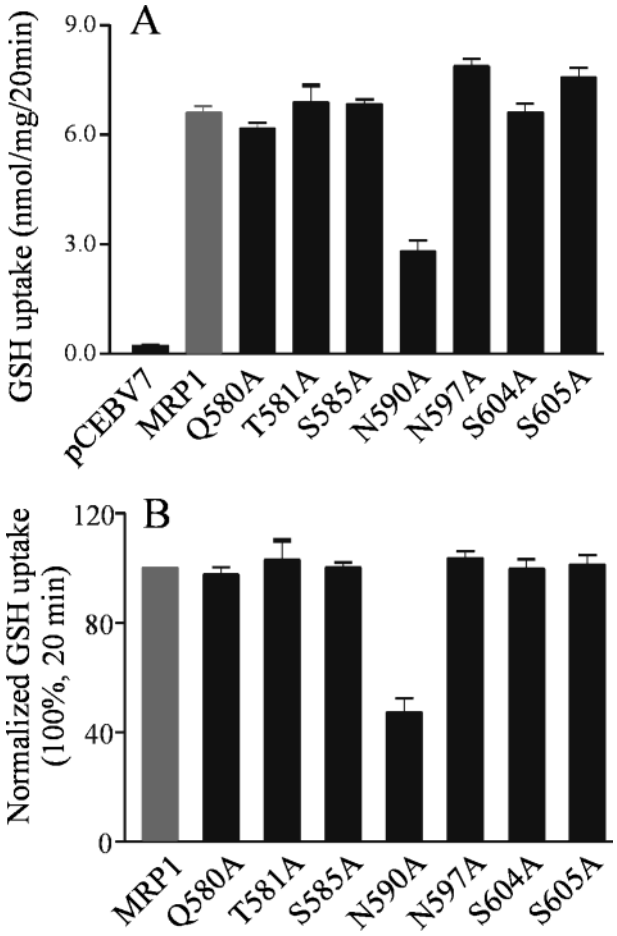

FIGURE 7: ATP-dependent verapamil-stimulated [^{3}H]GSH uptake by membrane vesicles prepared from HEK293 cells stably transfected with wild-type or mutant MRP1. Membrane vesicles were incubated at 37 °C with 100 μM GSH (300 nCi) in transport buffer in the presence of verapamil (100 μM) as described. Transfectants tested were expressing wild-type or mutant MRP1 as indicated in the figures. The normalized transport values were obtained by adjusting experimentally determined values (20 min time point) to compensate for differences in the relative levels of the wild-type and mutant proteins and are shown in panel B. Data shown in panel A have not been normalized to compensate for differences in expression levels. Values are mean ± SD of three independent experiments.

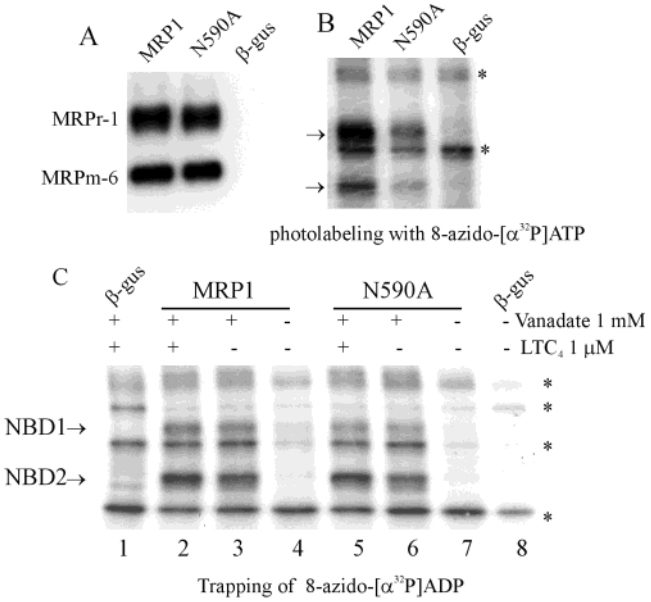

FIGURE 8: Photolabeling of wild-type and mutant MRP1 with 8-azido-[α**32**P]ATP and orthovanadate-induced trapping of 8-azido-[α**32**P]ATP by wild-type and mutant MRP1. Panel A: expression levels of the wild-type and mutant dual-half MRP1 proteins in membrane vesicles prepared from infected SF21 cells were determined by immunobloting and densitometry as described. Panel B: photolabeling of the wild-type and mutant dual-half proteins with 8-azido-[α^{32}P]ATP. Membrane proteins (20 μg) were incubated on ice with 1 μCi 8-azido-[α^{32}P]ATP, following the binding procedure as described. Similar results were obtained from two more experiments. Panel C: orthovanadate-induced trapping of 8-azido-[α^{32}P]ATP by wild-type and mutant MRP1. Membrane proteins (20 μg) were incubated with 1 μCi 8-azido-[α^{32}P]ATP, in the presence and absence of 1 μM LTC_4 at 37 °C for 15 min, following the trapping procedure as described. Similar results were obtained from two more experiments. An endogenous protein labeled is indicated by a star.

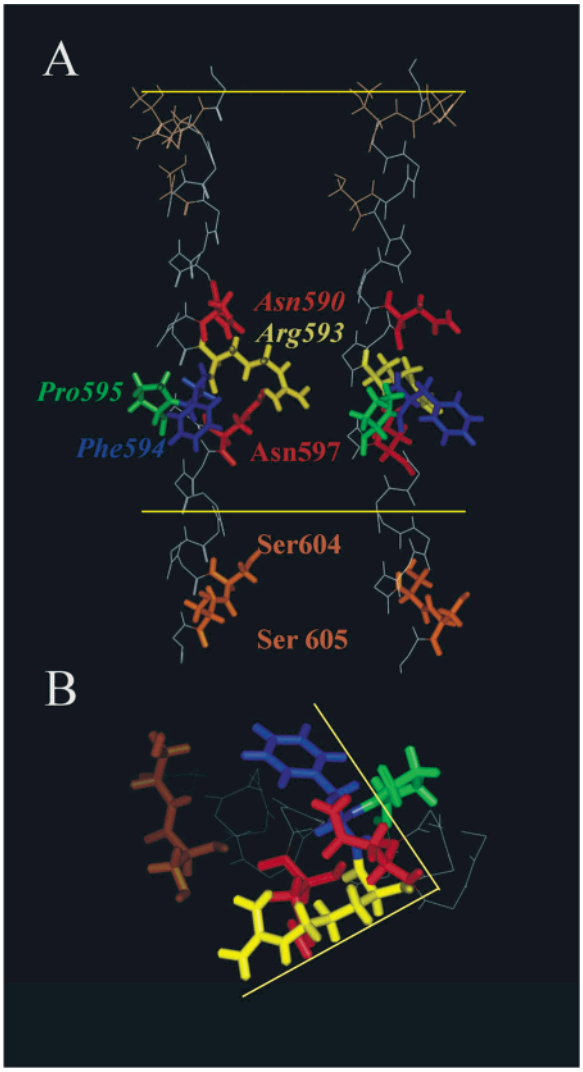

FIGURE 9: Predicted three-demensional structure for a segment of MRP1 from amino acids 579−606 derived from the model of MRP1 described by Campbell et al. (*48*). The views shown were generated using PyMol. Panel A shows two different views of TM11 with possible membrane interfaces indicated in yellow. The view on the right illustrates the kink in the helix introduced by Pro^{595}. Residues that affect the overall activity of the protein when nonconservatively mutated are shown in italics. Those that alter substrate specificity following nonconservative mutation are shown in normal font. Panel B represents a view from the extracellular side of the membrane down the axis of TM11. Amino acid residues are color-coded according to the scheme in panel A. The two yellow lines subtend an angle of 85° and bracket all mutation sensitive residues identified with the exception of Pro^{595}, which projects on the opposite face of the helix.

function tested. Mutation of Phe^{594} also markedly diminished photolabeling with LTC_4. However, unlike Asn^{590}, conservative substitution of Phe^{594} with Tyr or Trp altered the substrate specificity of the protein, suggesting that the latter residue may interact directly with substrate (*35*). Polar residues such as Asn, Gln, Asp, and Glu, located in transmembrane α-helices of multispanning TM proteins, have been shown to stabilize helix−helix interactions via interhelical hydrogen bonds (*56*−*58*). Given the pleiotropic effect of substitution of Asn^{590} with Ala and the lack of an effect of replacement with Asp or Gln, it appears likely that the hydrogen-bonding capacity of the side chain of the residue at position 590 may play a role in defining the conformation of the protein in the vicinity of the substrate binding pocket, possibly by interacting with residues in another helix. On the basis of our recently developed model of the tertiary structure of MSD2 and MSD3 of MRP1, such an interaction appears most likely to involve residues in TM6 and TM10 (*48*). The side chains of Lys^{332} and Asp^{336} in TM6 are predicted to be within 2−3 and 4−5 Å of the side chain of Asn^{590}, respectively. Interestingly, mutation of either of these two residues has a major effect on substrate specificity or overall activity (*50*). Nonconservative and conservative mutation of Lys^{332} selectively decreases the ability of the protein to bind and transport LTC_4, while both conservative and nonconservative mutations of Asp^{336} markedly decrease the overall activity of the protein (*49*, *50*).

The uniform effect of the N590A mutation on the relative efficiency of transport of several structurally diverse conjugated anions, as well as resistance to three different classes of drugs, suggested that it may have altered a common function, such as the coupling of transport to ATP hydrolysis or nucleotide binding and hydrolysis itself. In wild-type MRP, NBD1 binds ATP with relatively high affinity that, in turn, stimulates binding of ATP by NBD2 (*46*, *52*, *59*). We have also established that the binding of ATP by NBD2, rather than NBD1, actually drives the transition of the protein from a high- to low-affinity substrate binding state (*36*, *59*). Most recently, we reported that mutation of Asp^{1084}, predicted to be at/near the cytoplasm/membrane interface of TM14 of MRP1, dramatically decreased the binding and hydrolysis

of ATP at NBD2 without significant effect on the binding of ATP at NBD1. The D1084N mutation essentially eliminated the transport of LTC_4 and prevented the transition of the protein from a high- to low-affinity substrate binding state in the presence of ATP (*33*). The effect of the N590A mutation is less severe, and the mutant protein retains 30−40% of the transport activity of wild-type MRP1. Using dual expressed halves of the mutant protein, we were able to establish that in contrast to the Asp^{1084} mutation, the binding of ATP by NBD1 was markedly decreased, while the vanadate-dependent trapping of ADP by NBD2 was only weakly affected and remained responsive to the presence of the substrate, LTC_4. Thus, it appears likely that the reduction in transport in the N590A mutation is attributable to a decrease in the binding of ATP by NBD1 and a consequential reduction in ATP binding and hydrolysis at NBD2. A nonconservative mutation in CFTR, R347D, that results in a mild form of disease was recently found to affect the ATPase activity of the protein by decreasing its V_{max} for ATP 3−5-fold (*44*). R347D is predicted to be in the aqueous pore of the channel in the inner leaflet region of TM6. Arg^{347} of CFTR aligns with Arg^{593} in MRP1 mutation of which also decreases overall activity (*49*). Since there are many functional similarities between the cooperative interactions of the NBDs of MRP1 and CFTR, it is possible that the CFTR R347D mutation may be affecting the same step in the catalytic cycle as the N590A mutation.

There is now considerable experimental evidence that conformational changes of the NBDs both within and between the two domains upon nucleotide binding and hydrolysis result in significant reorientation of at least some of the TM helices in their associated MSDs. Similarly, changes in the orientation of certain TM helices may be capable of influencing the functional interactions between the NBDs that are required for ATP hydrolysis (*36*, *46*, *60*−*64*). It has been suggested based on the crystal structures of bacterial transporters such as MsbA and BtuCD that intracellular domains (ICDs) in contact with or connected to both TM helices and the NBDs may serve as bridges that transduce signals between NBD and TMDs (*65*−*67*). The predicted TM11 of MRP1 is directly connected to NBD1 by an intracellular domain corresponding to ICD3 of MsbA (Figure 1). Thus, changes in the position or orientation of TM11 caused by mutations, such as N590A, may be transmitted through the ICD causing a conformational or positional change in NBD1 that alters cooperativity between the two NBDs and results in diminished binding of ATP.

ACKNOWLEDGMENT

The authors thank Derek Shulze for advice on confocal microscopy.

REFERENCES

1. Cole, S. P. C., Bhardwaj, G., Gerlach, J. H., Mackie, J. E., Grant, C. E., Almquist, K. C., Stewart, A. J., Kurz, E. U., Duncan, A. M., and Deeley, R. G. (1992) Overexpression of a transporter gene in a multidrug-resistant human lung cancer cell line, *Science 258*, 1650−1654.
2. Borst, P., Evers, R., Kool, M., and Wijnholds, J. (2000) A family of drug transporters: the multidrug resistance-associated proteins, *J. Natl. Cancer Inst. 92*, 1295−1302.
3. Kao, H., Huang, J., and Chang, M. (2002) cDNA cloning and genomic organization of the murine MRP7, a new ATP-binding cassette transporter, *Gene 286*, 299−306.
4. Tammur, J., Prades, C., Arnould, I., Rzhetsky, A., Hutchinson, A., Adachi, M., Schuetz, J. D., Swoboda, K. J., Ptacek, L. J., Rosier, M., Dean, M., and Allikmets, R. (2001) Two new genes from the human ATP-binding cassette transporter superfamily, ABCC11 and ABCC12, tandemly duplicated on chromosome 16q12, *Gene 273*, 89−96.
5. Deeley, R. G., and Cole, S. P. C. (2002) Multidrug resistance protein 1 (ABCC1), in *ABC Proteins: From Bacteria to Man* (Holland, I., Cole, S. P., Kuchler, K., Higgins, C. F., Eds.) pp 39322, Academic Press, San Diego.
6. Higgins, C. F., Callaghan, R., Linton, K. J., Rosenberg, M. F., and Ford, R. C. (1997) Structure of the multidrug resistance *P*-glycoprotei, *Semin. Cancer Biol. 8*, 135−142.
7. Hipfner, D. R., Almquist, K. C., Leslie, E. M., Gerlach, J. H., Grant, C. E., Deeley, R. G., and Cole, S. P. C. (1997) Membrane topology of the multidrug resistance protein (MRP). A study of glycosylation-site mutants reveals an extracytosolic NH2 terminus, *J. Biol. Chem. 272*, 23623−23630.
8. Kast, C., and Gros, P. (1997) Topology mapping of the amino-terminal half of multidrug resistance-associated protein by epitope insertion and immunofluorescence, *J. Biol. Chem. 272*, 26479−26487.
9. Bakos, E., Hegedus, T., Hollo, Z., Welker, E., Tusnady, G. E., Zaman, G. J., Flens, M. J., Varadi, A., and Sarkadi, B. (1996) Membrane topology and glycosylation of the human multidrug resistance-associated protein, *J. Biol. Chem. 271*, 12322−12326.
10. Kast, C., and Gros, P. (1998) Epitope insertion favors a six transmembrane domain model for the carboxy-terminal portion of the multidrug resistance-associated protein, *Biochemistry 37*, 2305−2313.
11. Cole, S. P. C., Sparks, K. E., Fraser, K., Loe, D. W., Grant, C. E., Wilson, G. M., and Deeley, R. G. (1994) Pharmacological characterization of multidrug resistant MRP-transfected human tumor cells, *Cancer Res. 54*, 5902−5910.
12. Grant, C. E., Valdimarsson, G., Hipfner, D. R., Almquist, K. C., Cole, S. P. C., and Deeley, R. G. (1994) Overexpression of multidrug resistance-associated protein (MRP) increases resistance to natural product dru, *Cancer Res. 54*, 357−361.
13. Zaman, G. J., Flens, M. J., van Leusden, M. R., de Haas, M., Mulder, H. S., Lankelma, J., Pinedo, H. M., Scheper, R. J., Baas, F., and Broxterman, H. J. (1994) The human multidrug resistance-associated protein MRP is a plasma membrane drug-efflux pump, *Proc. Natl. Acad. Sci. U.S.A. 91*, 8822−8826.
14. Stride, B. D., Grant, C. E., Loe, D. W., Hipfner, D. R., Cole, S. P. C., and Deeley, R. G. (1997) Pharmacological characterization of the murine and human orthologs of multidrug-resistance protein in transfected human embryonic kidney cells, *Mol. Pharmacol. 52*, 344−353.
15. Breuninger, L. M., Paul, S., Gaughan, K., Miki, T., Chan, A., Aaronson, S. A., and Kruh, G. D. (1995) Expression of multidrug resistance-associated protein in NIH/3T3 cells confers multidrug resistance associated with increased drug efflux and altered intracellular drug distribution, *Cancer Res. 55*, 5342−5347.
16. Haimeur, A., Conseil, G., Deeley, R. G., and Cole, S. P. C. (2004) The MRP-related and BCRP/ABCG2 multidrug resistance proteins: biology, substrate specificity, and regulation, *Curr. Drug Metab. 5*, 21−53.
17. Ding, G. Y., Shen, T., and Center, M. S. (1999) Multidrug resistance-associated protein (MRP) mediated transport of daunomycin and leukotriene C4 (LTC_4) in isolated plasma membrane vesicles, *Anticancer Res. 19*, 3243−3248.
18. Renes, J., de Vries, E. G., Nienhuis, E. F., Jansen, P. L., and Muller, M. (1999) ATP- and glutathione-dependent transport of chemotherapeutic drugs by the multidrug resistance protein MRP1, *Br. J. Pharmacol. 126*, 681−688.
19. Loe, D. W., Almquist, K. C., Deeley, R. G., and Cole, S. P. C. (1996) Multidrug resistance protein (MRP)-mediated transport of leukotriene C4 and chemotherapeutic agents in membrane vesicles. Demonstration of glutathione-dependent vincristine transport, *J. Biol. Chem. 271*, 9675−9682.
20. Loe, D. W., Deeley, R. G., and Cole, S. P. C. (1998) Characterization of vincristine transport by the M(r) 190 000 multidrug resistance protein (MRP): evidence for cotransport with reduced glutathione, *Cancer Res. 58*, 5130−5136.
21. Mao, Q., Deeley, R. G., and Cole, S. P. C. (2000) Functional reconstitution of substrate transport by purified multidrug resistance protein MRP1 (ABCC1) in phospholipid vesicles, *J. Biol. Chem. 275*, 34166−34172.

22. Rappa, G., Lorico, A., Flavell, R. A., and Sartorelli, A. C. (1997) Evidence that the multidrug resistance protein (MRP) functions as a cotransporter of glutathione and natural product toxins, *Cancer Res. 57*, 5232−5237.
23. Loe, D. W., Almquist, K. C., Cole, S. P. C., and Deeley, R. G. (1996) ATP-dependent 17 β-estradiol 17-(β-D-glucuronide) transport by multidrug resistance protein (MRP). Inhibition by cholestatic steroids, *J. Biol. Chem. 271*, 9683−9689.
24. Leier, I., Jedlitschky, G., Buchholz, U., Cole, S. P. C., Deeley, R. G., and Keppler, D. (1994) The MRP gene encodes an ATP-dependent export pump for leukotriene C4 and structurally related conjugates, *J. Biol. Chem. 269*, 27807−27810.
25. Jedlitschky, G., Leier, I., Buchholz, U., Barnouin, K., Kurz, G., and Keppler, D. (1996) Transport of glutathione, glucuronate, and sulfate conjugates by the MRP gene-encoded conjugate export pump, *Cancer Res. 56*, 988−994.
26. Leier, I., Jedlitschky, G., Buchholz, U., Center, M., Cole, S. P. C, Deeley, R. G., and Keppler, D. (1996) ATP-dependent glutathione disulphide transport mediated by the MRP gene-encoded conjugate export pump, *Biochem. J. 314*, 433−437.
27. Muller, M., Meijer, C., Zaman, G. J., Borst, P., Scheper, R. J., Mulder, N. H., de Vries, E. G., and Jansen, P. L. (1994) Overexpression of the gene encoding the multidrug resistance-associated protein results in increased ATP-dependent glutathione *S*-conjugate transport, *Proc. Natl. Acad. Sci U.S.A. 91*, 13033−13037.
28. Qian, Y. M., Song, W. C., Cui, H., Cole, S. P. C., and Deeley, R. G. (2001) Glutathione stimulates sulfated estrogen transport by multidrug resistance protein 1, *J. Biol. Chem. 276*, 6404−6411.
29. Leslie, E. M., Ito, K., Upadhyaya, P., Hecht, S. S., Deeley, R. G., and Cole, S. P. C. (2001) Transport of the β-*O*-glucuronide conjugate of the tobacco-specific carcinogen 4-(methylnitrosamino)-1-(3-pyridyl)-1-butanol (NNAL) by the multidrug resistance protein 1 (MRP1). Requirement for glutathione or a non-sulfur-containing analogue, *J. Biol. Chem. 276*, 27846−27854.
30. Zhang, D. W., Cole, S. P. C., and Deeley, R. G. (2002) Determinants of the substrate specificity of multidrug resistance protein 1: role of amino acid residues with hydrogen-bonding potential in predicted transmembrane helix 17, *J. Biol. Chem. 277*, 20934−20941.
31. Zhang, D. W., Cole, S. P. C., and Deeley, R. G. (2001) Identification of a nonconserved amino acid residue in multidrug resistance protein 1 important for determining substrate specificity: evidence for functional interaction between transmembrane helices 14 and 17, *J. Biol. Chem. 276*, 34966−34974.
32. Ito, K., Olsen, S. L., Qiu, W., Deeley, R. G., and Cole, S. P. C. (2001) Mutation of a single conserved tryptophan in multidrug resistance protein 1 (MRP1/ABCC1) results in loss of drug resistance and selective loss of organic anion transport, *J. Biol. Chem. 276*, 15616−15624.
33. Zhang, D. W., Gu, H. M., Situ, D., Haimeur, A., Cole, S. P. C, and Deeley, R. G. (2003) Functional importance of polar and charged amino acid residues in transmembrane helix 14 of multidrug resistance protein 1 (MRP1/ABCC1): identification of an aspartate residue critical for conversion from a high to low affinity substrate binding state, *J. Biol. Chem. 278*, 46052−46063.
34. Ren, X. Q., Furukawa, T., Aoki, S., Sumizawa, T., Haraguchi, M., Nakajima, Y., Ikeda, R., Kobayashi, M., and Akiyama, S. I. (2002) A positively charged amino acid proximal to the C-terminus of TM17 of MRP1 is indispensable for GSH-dependent binding of substrates and for transport of LTC4, *Biochemistry 41*, 14132−14140.
35. Koike, K., Conseil, G., Leslie, E., Deeley, R. G., and Cole, S. P. C. (2004) Identification of proline residues in the core cytoplasmic and transmembrane regions of multidrug resistance protein 1 (MRP1/ABCC1) important for transport function, substrate specificity, and nucleotide interactions, *J. Biol. Chem. 279*, 12325−12336.
36. Qian, Y. M., Qiu, W., Gao, M., Westlake, C. J., Cole, S. P. C., and Deeley, R. G. (2001) Characterization of binding of leukotriene C4 by human multidrug resistance protein 1: evidence of differential interactions with NH2- and COOH-proximal halves of the protein, *J. Biol. Chem. 276*, 38636−38644.
37. Mao, Q., Qiu, W., Weigl, K. E., Lander, P. A., Tabas, L. B., Shephard, R. L., Dantzig, A. H., Deeley, R. G., and Cole, S. P. C. (2002) GSH-dependent photolabeling of multidrug resistance protein MRP1 (ABCC1) by [^{125}I]LY475776. Evidence of a major binding site in the COOH-proximal membrane spanning domain, *J. Biol. Chem. 277*, 28690−28699.
38. Qian, Y. M., Grant, C. E., Westlake, C. J., Zhang, D. W., Lander, P. A., Shepard, R. L., Dantzig, A. H., Cole, S. P. C., and Deeley, R. G. (2002) Photolabeling of human and murine multidrug resistance protein 1 with the high affinity inhibitor [^{125}I]LY475776 and azidophenacyl-[^{35}S]glutathione, *J. Biol. Chem. 277*, 35225−35231.
39. Daoud, R., Julien, M., Gros, P., and Georges, E. (2001) Major photoaffinity drug binding sites in multidrug resistance protein 1 (MRP1) are within transmembrane domains 10−11 and 16−17, *J. Biol. Chem. 276*, 12324−12330.
40. Loo, T. W., Bartlett, M. C., and Clarke, D. M. (2003) Methanethiosulfonate derivatives of rhodamine and verapamil activate human *P*-glycoprotein at different site, *J. Biol. Chem. 278*, 50136−50141.
41. Zhou, Y., Gottesman, M. M., and Pastan, I. (1999) Domain exchangeability between the multidrug transporter (MDR1) and phosphatidylcholine flippase (MDR2), *Mol. Pharmacol. 56*, 997−1004.
42. McCarty, N. A., and Zhang, Z. R. (2001) Identification of a region of strong discrimination in the pore of CFTR, *Am. J. Physiol. Lung Cell Mol. Physiol. 281*, L852−867.
43. Gupta, J., and Lindsell, P. (2003) Extent of the selectivity filter conferred by the sixth transmembrane region in the CFTR chloride channel pore, *Mol. Membr. Biol. 20*, 45−52.
44. Kogan, I., Ramjeesingh, M., Huan, L. J., Wang, Y., and Bear, C. E. (2001) Perturbation of the pore of the cystic fibrosis transmembrane conductance regulator (CFTR) inhibits its ATPase activity, *J. Biol. Chem. 276*, 11575−11581.
45. Zhang, D. W., Cole, S. P. C., and Deeley, R. G. (2001) Identification of an amino acid residue in multidrug resistance protein 1 critical for conferring resistance to anthracyclines, *J. Biol. Chem. 276*, 13231−13239.
46. Gao, M., Cui, H. R., Loe, D. W., Grant, C. E., Almquist, K. C., Cole, S. P. C., and Deeley, R. G. (2000) Comparison of the functional characteristics of the nucleotide binding domains of multidrug resistance protein 1, *J. Biol. Chem. 275*, 13098−13108.
47. Stride, B. D., Cole, S. P. C., and Deeley, R. G. (1999) Localization of a substrate specificity domain in the multidrug resistance protein, *J. Biol. Chem. 274*, 22877−22883.
48. Campbell, J. D., Koike, K., Moreau, C., Sansom, M. S., Deeley, R. G., and Cole, S. P. C. (2004) Molecular modeling correctly predicts the functional importance of Phe594 in transmembrane helix 11 of the multidrug resistance protein, MRP1 (ABCC1), *J. Biol. Chem. 279*, 463−468.
49. Haimeur, A., Conseil, G., Deeley, R. G., and Cole, S. P. C. (2004) Mutations of Charged Amino Acids in or Proximal to the Transmembrane Helices of the Second Membrane Spanning Domain Differentially Affect the Substrate Specificity and Transport Activity of Human Multidrug Resistance Protein, MRP1 (ABCC1), *Mol. Pharm., 65*, 1375−1385.
50. Haimeur, A., Deeley, R. G., and Cole, S. P. C. (2002) Charged amino acids in the sixth transmembrane helix of multidrug resistance protein 1 (MRP1/ABCC1) are critical determinants of transport activity, *J. Biol. Chem.* 277, 41326−41333.
51. Loe, D. W., Deeley, R. G., and Cole, S. P. C. (2000) Verapamil stimulates glutathione transport by the 190 kDa multidrug resistance protein 1 (MRP1), *J. Pharmacol. Exp. Ther. 293*, 530−538.
52. Hou, Y. X., Cui, L., Riordan, J. R., and Chang, X. B. (2002) ATP binding to the first nucleotide-binding domain of multidrug resistance protein MRP1 increases binding and hydrolysis of ATP and trapping of ADP at the second domain, *J. Biol. Chem. 277*, 5110−5119.
53. Poelarends, G. J., and Konings, W. N. (2002) The transmembrane domains of the ABC multidrug transporter LmrA form a cytoplasmic exposed, aqueous chamber within the membrane, *J. Biol. Chem. 277*, 42891−42898.
54. Taguchi, Y., Kino, K., Morishima, M., Komano, T., Kane, S. E., and Ueda, K. (1997) Alteration of substrate specificity by mutations at the His61 position in predicted transmembrane domain 1 of human MDR1/P-glycoprotein, *Biochemistry 36*, 8883−8889.
55. Zhang, D. W., Gu, H. M., Vasa, M., Muredda, M., Cole, S. P. C, and Deeley, R. G. (2003) Characterization of the role of polar amino acid residues within predicted transmembrane helix 17 in determining the substrate specificity of multidrug resistance protein 3, *Biochemistry 42*, 9989−10000.
56. Partridge, A. W., Melnyk, R. A., and Deber, C. M. (2002) Polar residues in membrane domains of proteins: molecular basis for

helix−helix association in a mutant CFTR transmembrane segment, *Biochemistry 41*, 3647−3653.
57. Gratkowski, H., Lear, J. D., and DeGrado, W. F. (2001) Polar side chains drive the association of model transmembrane peptides, *Proc. Natl. Acad. Sci. U.S.A. 98*, 880−885.
58. Zhou, F. X., Merianos, H. J., Brunger, A. T., and Engelman, D. M. (2001) Polar residues drive association of polyleucine transmembrane helices, *Proc. Natl. Acad. Sci. U.S.A. 98*, 2250−2255.
59. Payen L. F., Gao M., Westlake C. J., Cole S. P., and Deeley, R. G. (2003) Role of carboxylate residues adjacent to the conserved core Walker B motifs in the catalytic cycle of multidrug resistance protein 1 (ABCC1), *J. Biol. Chem. 278*, 38537−38547.
60. Koike, K., Oleschuk, C. J., Haimeur, A., Olsen, S. L., Deeley, R. G., and Cole, S. P. (2002) Multiple membrane-associated tryptophan residues contribute to the transport activity and substrate specificity of the human multidrug resistance protein, MRP1, *J. Biol. Chem. 277*, 49495−49503.
61. Hou, Y., Cui, L., Riordan, J. R., and Chang, X. (2000) Allosteric interactions between the two nonequivalent nucleotide binding domains of multidrug resistance protein MRP1, *J. Biol. Chem. 275*, 20280−20287.
62. Loo, T. W., and Clarke, D. M. (2002) Vanadate trapping of nucleotide at the ATP-binding sites of human multidrug resistance *P*-glycoprotein exposes different residues to the drug-binding site, *Proc. Natl. Acad. Sci. U.S.A. 99*, 3511−3516.
63. Loo, T. W., Bartlett, M. C., and Clarke, D. M. (2003) Drug binding in human *P*-glycoprotein causes conformational changes in both nucleotide-binding domains, *J. Biol. Chem. 278*, 1575−1578.
64. Jones, P. M., and George, A. M. (2002) Mechanism of ABC transporters: a molecular dynamics simulation of a well-characterized nucleotide-binding subunit, *Proc. Natl. Acad. Sci. U.S.A.* 99, 12639−12644.
65. Chang, G., and Roth, C. B. (2001) Structure of MsbA from *E. coli*: a homologue of the multidrug resistance ATP binding cassette (ABC) transporters, *Science 293*, 1793−1800.
66. Chang, G. (2003) Structure of MsbA from Vibrio cholera: a multidrug resistance ABC transporter homologue in a closed conformation, *J. Mol. Biol*. *330*, 419−430.
67. Locher, K. P., Lee, A. T., and Rees, D. C. (2002) The *E. coli* BtuCD structure: a framework for ABC transporter architecture and mechanism, *Science 296*, 1091−1098.

BI0495230